

# On the enrichment zone size for optimal convergence rate of the Generalized/Extended Finite Element Method



Varun Gupta<sup>a</sup>, C. Armando Duarte<sup>b,\*</sup>

<sup>a</sup> Advanced Computing, Mathematics and Data Division, Pacific Northwest National Laboratory, 902 Battelle Boulevard, P.O. Box 999, MSIN K7-90, Richland, WA 99352, USA

<sup>b</sup> Department of Civil and Environmental Engineering, University of Illinois at Urbana-Champaign, Newmark Laboratory, 205 North Mathews Avenue, Urbana, IL 61801, USA

## ARTICLE INFO

### Article history:

Received 17 February 2016

Accepted 30 April 2016

Available online 1 June 2016

### Keywords:

GFEM

XFEM

Fracture mechanics

Cracks

Singularity

## ABSTRACT

Singular enrichment functions are broadly used in Generalized or Extended Finite Element Methods (GFEM/XFEM) for linear elastic fracture mechanics problems. These functions are used at finite element nodes within an enrichment zone around the crack tip/front in 2- and 3-D problems, respectively. Small zones lead to suboptimal convergence rate of the method while large ones lead to ill-conditioning of the system of equations and to a large number of degrees of freedom. This paper presents an *a priori* estimate for the minimum size of the enrichment zone required for optimal convergence rate of the GFEM/XFEM. The estimate shows that the minimum size of the enrichment zone for optimal convergence rate depends on the element size and polynomial order of the GFEM/XFEM shape functions. Detailed numerical verification of these findings is also presented.

© 2016 Elsevier Ltd. All rights reserved.

## 1. Introduction

The advent of Partition of Unity methods [1,2], like the *hp*-cloud method [3,2,4], the Generalized or Extended Finite Element Method (GFEM/XFEM) [5,6,1,7–9], and the Particle Partition of Unity Method [10,11], has greatly facilitated the computation of accurate and efficient numerical solutions for problems with singularities. Of particular engineering relevance are linear elastic fracture mechanics problems with stationary or propagating cracks. The rapid growth and development of the GFEM/XFEM in the last two decades has led to a phenomenal increase in the number of users of these methods and its availability in mainstream commercial finite element software like Abaqus [12] and LS-DYNA [13]. The main idea behind the GFEM/XFEM is to incorporate *a priori* knowledge about the solution of a problem into the finite element solution space using the partition of unity property of finite element shape functions. It is to be noted that GFEM and XFEM are essentially the same methods, as discussed in [14]. The names GFEM and XFEM are used interchangeably in this paper.

Several researchers have exploited the robustness and flexibility associated with the GFEM/XFEM to solve elasticity problems involving cracks [15–20]. This method relaxes meshing constraints imposed by the standard Finite Element Method (FEM) for modeling cracks or moving interfaces. In addition, it improves the numerical accuracy while retaining the attractive features of the FEM. In problems involving cracks, the singularity is resolved poorly by the polynomial shape functions used in the FEM, unless a highly-refined mesh is used close to the crack tip. The GFEM alleviates this problem by building a solution space containing *a priori* knowledge about the elasticity solution in the neighborhood of cracks.

\* Corresponding author.

E-mail address: [caduarte@illinois.edu](mailto:caduarte@illinois.edu) (C.A. Duarte).

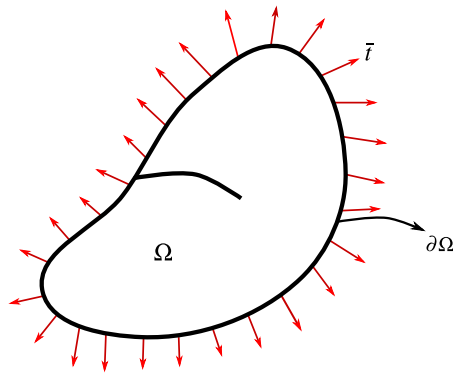


Fig. 1. Linear elastic boundary value problem with a crack in 2-D.

The GFEM can handle discontinuities and singularities independently of the finite element mesh by proper selection of local approximation spaces in pre-selected regions of the problem domain. This is accomplished through the so-called *enrichment functions*. For problems involving cracks, two types of enrichment functions are typically adopted [21,19,22]: (i) Heaviside functions able to represent the discontinuity of the elasticity solution across the crack surface and (ii) Westergaard asymptotic singular displacement fields, which approximate the singularity and discontinuity of the elasticity solution near the crack tip.

Most GFEM formulations for fractures [15,21,19] have adopted singular enrichment functions only at the nodes of elements containing the crack tip in 2-D or intersected by the crack front in 3-D. This enrichment strategy, referred to as *topological enrichment* [23,24], leads to the same suboptimal convergence behavior as the standard FEM on quasi-uniform meshes. Laborde et al. [23] and Béchet et al. [24] proposed the idea of enriching finite element nodes in a fixed neighborhood around the crack tip/front. This so-called *geometrical enrichment* strategy leads to optimal convergence rate, as in problems with smooth solutions, provided proper singular enrichment functions are adopted [25]. A brief overview of these enrichment strategies is presented in Section 4. Other researchers [26,27] have also numerically demonstrated the need for geometrical enrichment around the crack tip/front in order to obtain optimal convergence rate.

The geometrical *enrichment zone* with singular enrichment functions can be chosen arbitrarily large. However, large enrichment zones lead to ill-conditioned stiffness matrices as shown in [28,29] and to a larger number of degrees of freedom than the topological enrichment strategy. Therefore, estimates of the minimum size of the enrichment zone required for optimal convergence rate of the GFEM are needed. To the authors' knowledge, no guidelines for the selection of enrichment zone sizes in the GFEM/XFEM are available in the literature. This paper presents an *a priori* estimate for the minimum size of the enrichment zone. The estimate shows that the minimum size depends on the element size and polynomial order of the GFEM shape functions. Numerical verification of these findings is also presented.

After this introduction, Section 2 describes the linear elastic fracture mechanics problem considered in this study, followed by a brief review of the Generalized Finite Element Method (GFEM) in Section 3. Section 4 reviews enrichment strategies commonly adopted in the neighborhood of a crack tip. Section 4.3 presents an *a priori* estimate of the minimum size of the enrichment zone for linear elastic fracture mechanics problems. Numerical experiments aimed at the verification of the proposed estimate are presented in Section 5. Finally, Section 6 summarizes the main results and conclusions of this study.

## 2. Model problem definition

Consider a cracked domain,  $\bar{\Omega} = \Omega \cup \partial\Omega$  in  $\mathbb{R}^2$ , like the one shown in Fig. 1.

The equilibrium and constitutive equations are given by

$$\nabla \cdot \boldsymbol{\sigma} = \mathbf{0} \quad \boldsymbol{\sigma} = \mathbf{C} : \boldsymbol{\varepsilon} \quad \text{in } \Omega \quad (1)$$

where  $\mathbf{C}$  is Hooke's tensor,  $\boldsymbol{\sigma}$  denotes the Cauchy stress tensor, and  $\boldsymbol{\varepsilon}$  is the small strain tensor. The following boundary conditions are prescribed on  $\partial\Omega$

$$\boldsymbol{\sigma} \cdot \mathbf{n} = \bar{\mathbf{t}} \quad \text{on } \partial\Omega \quad (2)$$

where  $\mathbf{n}$  is the outward unit normal vector to  $\partial\Omega$  and  $\bar{\mathbf{t}}$  are prescribed tractions. The crack surface is assumed to be traction-free, i.e.,  $\bar{\mathbf{t}} = \mathbf{0}$  on the crack surface. Eqs. (1) and (2) are the strong form of governing equations.

The weak formulation of the problem above is given by the Principle of Virtual Work, which reads

Find  $\mathbf{u} \in \mathcal{E}(\Omega)$ , such that  $\forall \mathbf{v} \in \mathcal{E}(\Omega)$

$$B(\mathbf{u}, \mathbf{v}) = F(\mathbf{v}) \quad (3)$$

where

$$B(\mathbf{u}, \mathbf{v}) = \int_{\Omega} \boldsymbol{\sigma}(\mathbf{u}) : \boldsymbol{\varepsilon}(\mathbf{v}) dA$$

$$F(\mathbf{v}) = \int_{\partial\Omega} \bar{\mathbf{t}} \cdot \mathbf{v} ds$$

and  $\mathcal{E}(\Omega)$  is the energy space [30] with norm

$$\| \cdot \|_{\mathcal{E}(\Omega)} = \sqrt{B(\cdot, \cdot)}. \tag{4}$$

Numerical approximations to the solution of Problem (3) are computed in Section 5 using the Galerkin method with discretization spaces as described in Section 3.

### 3. Generalized finite element approximations

Let  $\mathbf{u}_h$  denote a generalized FEM approximation of the exact solution  $\mathbf{u}$  of the problem given by (3). From the Principle of Virtual Work and Galerkin’s method, it can be shown that the approximation  $\mathbf{u}_h$  is the solution of the problem

Find  $\mathbf{u}_h \in \mathbb{S}_{GFEM}(\Omega) \subset \mathcal{E}(\Omega)$ , such that  $\forall \mathbf{v}_h \in \mathbb{S}_{GFEM}(\Omega)$

$$\int_{\Omega} \boldsymbol{\sigma}(\mathbf{u}_h) : \boldsymbol{\varepsilon}(\mathbf{v}_h) d\mathbf{x} = \int_{\partial\Omega} \bar{\mathbf{t}} \cdot \mathbf{v}_h ds \tag{5}$$

where  $\mathbb{S}_{GFEM}(\Omega)$  is a discretization of the energy space  $\mathcal{E}(\Omega)$  defined on  $\Omega$  and built with generalized FEM shape functions. The GFEM space  $\mathbb{S}_{GFEM}$  is typically defined on quasi-uniform finite element meshes using the concept of a partition of unity as described below. This leads to a system of linear equations to be solved for the unknown degrees of freedom of  $\mathbf{u}_h$ .

A generalized finite element shape function  $\phi_{\alpha i}(\mathbf{x})$  is built from the product of a standard Lagrangian finite element shape function  $N_{\alpha}(\mathbf{x})$  and an enrichment function  $L_{\alpha i}(\mathbf{x})$ , i.e.,

$$\phi_{\alpha i}(\mathbf{x}) = N_{\alpha}(\mathbf{x})L_{\alpha i}(\mathbf{x}) \tag{6}$$

where  $\alpha \in I_h^e \subset I_h = \{1, \dots, n\}$  is the index of a node in a FE mesh and  $i \in \mathcal{I}(\alpha) = \{1, \dots, m_{\alpha}\}$  is the index of the enrichment function at the node. In this paper,  $N_{\alpha}$ ,  $\alpha \in I_h$ , are linear functions. The support of  $N_{\alpha}(\mathbf{x})$ , denoted by  $\bar{\omega}_{\alpha}$ , is given by the union of all the finite elements sharing node  $\alpha$ . The enrichment functions  $\{L_{\alpha i}\}_{i=1}^{m_{\alpha}}$  form a basis of a local space  $\chi_{\alpha}(\omega_{\alpha})$ . It is noted that the FE shape functions form a partition of unity, i.e.,  $\sum_{\alpha \in I_h} N_{\alpha}(\mathbf{x}) = 1$ ,  $\mathbf{x} \in \Omega$ .

The test and trial GFEM space  $\mathbb{S}_{GFEM}$  is given by

$$\mathbb{S}_{GFEM} = \mathbb{S}_{FEM} + \mathbb{S}_{ENR} \tag{7}$$

where

$$\mathbb{S}_{FEM} = \sum_{\alpha \in I_h} c_{\alpha} N_{\alpha}, \quad c_{\alpha} \in \mathbb{R},$$

$$\text{and } \mathbb{S}_{ENR} = \sum_{\alpha \in I_h^e \subset I_h} N_{\alpha} \chi_{\alpha}; \quad \chi_{\alpha} = \text{span}\{L_{\alpha i}\}_{i=1}^{m_{\alpha}}. \tag{8}$$

The shape functions in  $\mathbb{S}_{ENR}$  are computed using (6). Fig. 2 illustrates their construction in a two-dimensional domain: Fig. 2(a) for a polynomial enrichment function and Fig. 2(b) for a non-polynomial enrichment function.

The selection of enrichment functions based on *a priori* knowledge about the solution of a problem is the key concept in partition of unity methods like the GFEM. When polynomial functions are adopted for the basis of local spaces  $\chi_{\alpha}(\omega_{\alpha})$ ,  $\alpha \in I_h^e$ , the GFEM space  $\mathbb{S}_{GFEM}$  is analogous, but not identical, to that provided by high-order FEM. The main strength of the GFEM is its ability to adopt non-polynomial enrichment functions which can locally approximate the solution over  $\omega_{\alpha}$ ,  $\alpha \in I_h^e$ . The partition of unity is used to patch together the local approximation spaces. The reader is referred to [5,6,1,7] for further details and properties of the GFEM.

### 4. Selection of enrichment zone $I_h^e$

Singular enrichment functions for the model problem of Section 2 are provided by the asymptotic expansion of the 2-D elasticity solution in the neighborhood of a crack [30]. In particular, we adopt the first term of the Mode I and Mode II expansions. They are given in (21) and (23), respectively. These functions are used at local spaces  $\chi_{\alpha}$ ,  $\alpha \in I_h^e \subset I_h$ . The set  $I_h^e$  typically corresponds to finite element nodes in a neighborhood of the crack, where the asymptotic expansion is valid. Fig. 7 illustrates this set for our model problem. However, the selection of this *enrichment zone* is up to the user of the GFEM. The next section discusses two approaches proposed in the literature for the selection of  $I_h^e$ . It is noted that Heaviside functions are not adopted as enrichments in this work. All nodes in set  $I_h^e$  have functions defined in (21) and (23).

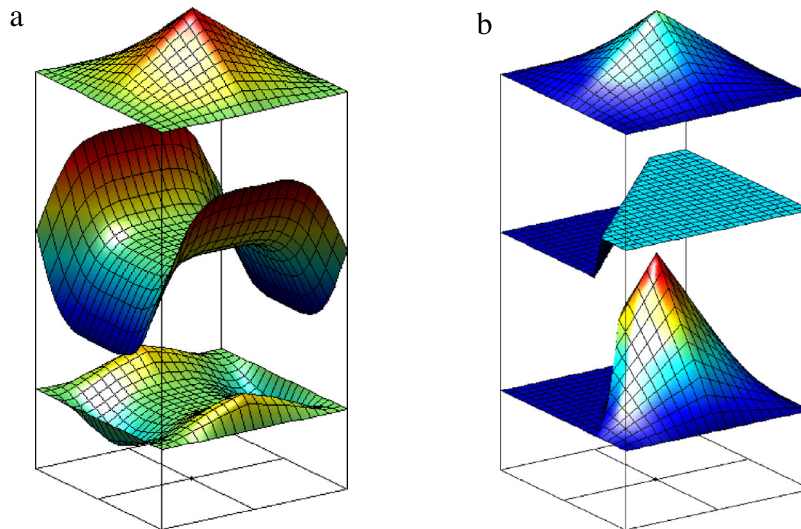


**Fig. 2.** Construction of a generalized FEM shape function using a polynomial (a) and a non-polynomial (b) enrichment. Here,  $N_{\alpha}$  is the function at the top, the enrichment function,  $L_{\alpha i}$ , is the function in the middle, and the generalized FE shape function,  $\phi_{\alpha i}$ , is the resulting shape function shown at the bottom.

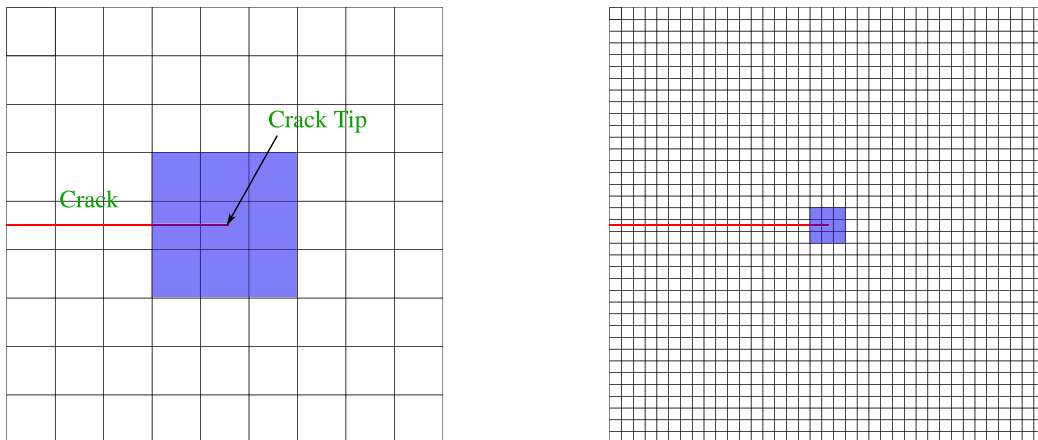


**Fig. 3.** Topological enrichment around a crack tip in 2-D. The size of the enrichment zone goes to zero with mesh refinement.

#### 4.1. Topological enrichment

In this enrichment strategy, set  $I_h^e$  corresponds to nodes of finite elements intersected by the crack front. In this strategy, the size of the enrichment region goes to zero as the mesh is refined close to the crack front. As a result, it leads to the same poor convergence rate as in the finite element on quasi-uniform meshes [24,23,26]. Fig. 3 illustrates this strategy. Topological enrichment is broadly used in the literature, in particular when solving 3-D problems.

#### 4.2. Geometrical enrichment

In this enrichment strategy, set  $I_h^e$  corresponds to all nodes within a prescribed distance  $d$  from the crack front, regardless of the mesh size [24,23]. As a result, the elasticity solution is well captured in the neighborhood of the crack. The GFEM attains optimal convergence rate, i.e., the same rate as in problems with smooth solutions, *even on uniform meshes* [25,28,29]. Fig. 4 illustrates the geometrical enrichment strategy in a 2-D setting. The main drawbacks of the geometrical enrichment are the large number of degrees of freedom and the ill-conditioning of the GFEM stiffness matrices [28]. These issues are particularly severe in 3-D problems [29]. Therefore, estimates of the minimum size of the enrichment zone able to deliver optimal convergence rate are of practical relevance.

#### 4.3. Minimum size of the enrichment zone for optimal convergence

In this section, we analyze the geometrical enrichment strategy described above. Our goal is to find the conditions under which that strategy leads to optimal convergence rate in the  $h$ -version of the GFEM. We show that the minimal size of the

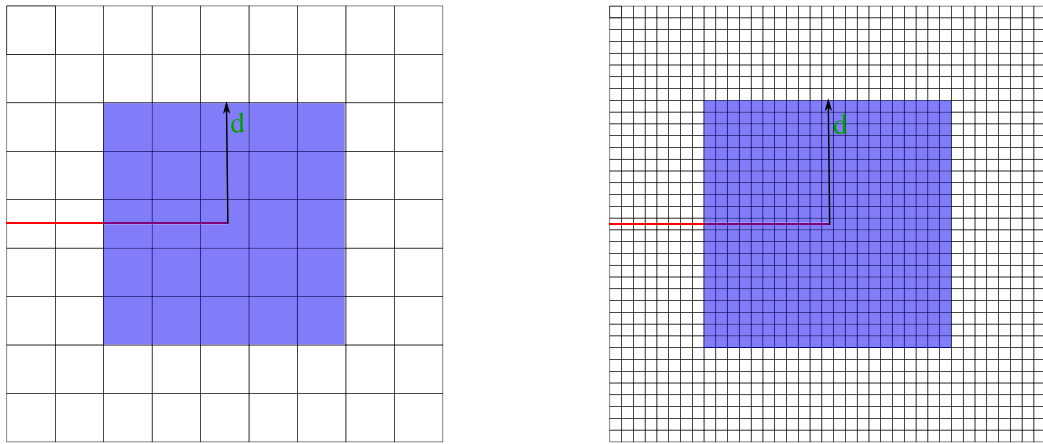


**Fig. 4.** Geometrical enrichment defined on a square region of edge size  $2d$  around a crack tip in 2-D. The size of the enrichment zone is independent of the finite element mesh.

enrichment zone is dependent on the element size and polynomial approximation order. The focus is on the model problem of Section 2.

The convergence of the  $h$ -version of the finite element method is governed by [30]

$$\|\mathbf{u} - \mathbf{u}_h\|_{H^1(\Omega)} = \|\mathbf{e}\|_{H^1(\Omega)} \leq Ch^{\min(p,k-1)} \|\mathbf{u}\|_{H^k(\Omega)} \tag{9}$$

where [31]

$$\|\mathbf{u}\|_{H^k(\Omega)}^2 = \sum_{0 \leq |\gamma| \leq k} \iint_{\Omega} |D^\gamma \mathbf{u}|^2 dx_1 dx_2; \quad \text{with } \gamma = \langle \gamma_1, \gamma_2 \rangle, \quad D^\gamma = \left( \frac{\partial}{\partial x_1} \right)^{\gamma_1} \left( \frac{\partial}{\partial x_2} \right)^{\gamma_2} \tag{10}$$

and

$\mathbf{u}$  and  $\mathbf{u}_h$  are the exact and FEM solutions, respectively,  
 $C$  is a constant independent of  $\mathbf{u}$  and  $h$ , the size of the largest finite element in the mesh,  
 $p$  is the polynomial order of the FEM shape functions, and  
 $k$  denotes the order of the Hilbert space  $H^k(\Omega)$  to which the exact solution belongs, which in turn is a measure of the smoothness of the solution  $\mathbf{u}$ .

The convergence of the  $h$ -version of the generalized finite element method is also governed by (9) if topological enrichment is adopted or if only polynomial functions are used for the basis of the local spaces  $\chi_\alpha, \alpha \in I_h^e$  [1,32].

The first term of the Mode I and II expansions of the solution of our model problem in the neighborhood of the crack are provided by (21) and (23), respectively. The smoothness of these functions is controlled by the  $\sqrt{r}$  term. This function is plotted in Fig. 5. The horizontal axis in the figure has the distance  $r$  from the crack tip.

Suppose that a uniform mesh with elements of size  $h$  has a circular geometrical enrichment of radius  $d$  around the crack tip. If the local spaces  $\chi_\alpha, \alpha \in I_h^e$ , can approximate the exact solution well, the convergence rate of the GFEM solution is controlled by the error outside of the enrichment zone. In the case of our model problem, the convergence rate is controlled by the error in the elements immediately outside of the enrichment zone. The region with these elements is indicated by  $\Omega_e^*$  in Fig. 5. This is the case since the solution farther away from the enrichment zone is smoother than in  $\Omega_e^*$ .

Our goal is to find the dimension  $d$  shown in Fig. 5, such that the convergence rate of the  $h$ -version of the GFEM is optimal, i.e., equal to the polynomial order of the shape functions. According to (9) and the discussion above, this will be the case if the restriction of the solution  $\mathbf{u}$  to  $\Omega_e^*$  belongs to the Hilbert space of order  $p + 1$ , i.e.,

$$\mathbf{u}|_{\Omega_e^*} \in H^{(p+1)}(\Omega_e^*). \tag{11}$$

Using the above and (9), we get

$$\|\mathbf{e}\|_{H^1(\Omega_e^*)} \leq Ch^p \|\mathbf{u}\|_{H^{p+1}(\Omega_e^*)} \tag{12}$$

where  $C$  is independent of  $\mathbf{u}$  and  $h$ . Eq. (12) implies that the convergence rate will be optimal and equal to  $p$  if  $h$  and  $d$  are selected so that  $\|\mathbf{u}\|_{H^{p+1}(\Omega_e^*)}$  is bounded by a constant.

The first term of the Mode I and II expansions of the 2-D elasticity solution in the neighborhood of a crack can be written, according to (21) and (23), as

$$\mathbf{u}(r, \theta) = (u_{x1}(r, \theta), u_{x2}(r, \theta)) = r^{\frac{1}{2}} \mathbf{f}(\theta) \tag{13}$$

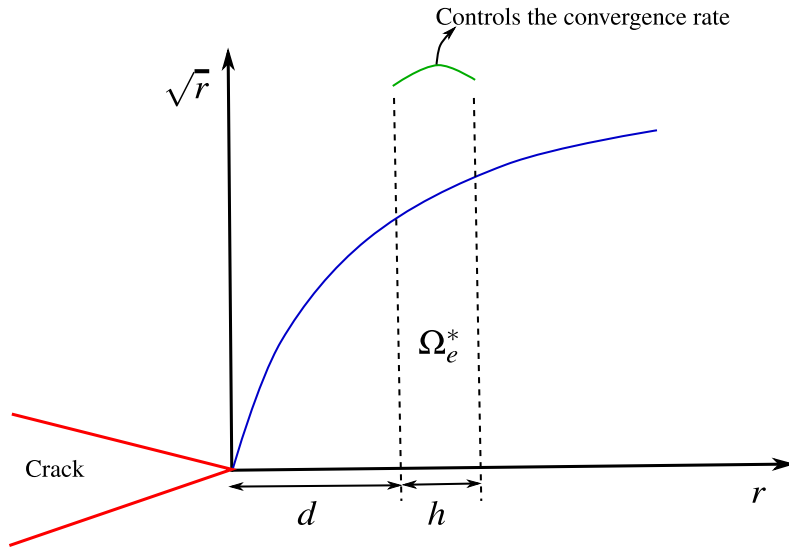


Fig. 5. Behavior of near crack tip displacement field.

where  $r$  is the distance from the crack tip and  $\mathbf{f}(\theta) = (f_{x1}(\theta), f_{x2}(\theta))$  is a smooth function of the polar coordinate  $\theta$ . Second and higher order terms of the elasticity expansion are smoother than the first one. The  $(p + 1)$ th derivative of (13) with respect to  $r$  is given by

$$\frac{\partial^{p+1} \mathbf{u}}{\partial r^{p+1}} = r^{-\frac{1}{2}-p} \mathbf{f}(\theta). \tag{14}$$

From the definition of the Sobolev norm,  $\|\mathbf{u}\|_{H^{p+1}(\Omega_e^*)}$  can be written as (see Eq. (10)),

$$\|\mathbf{u}\|_{H^{p+1}(\Omega_e^*)}^2 = \sum_{0 \leq |\gamma| \leq p+1} \iint_{\Omega_e^*} |D^\gamma \mathbf{u}|^2 dx_1 dx_2. \tag{15}$$

Now,

$$\begin{aligned} \iint_{\Omega_e^*} |D^\gamma \mathbf{u}|^2 dx_1 dx_2 &\leq \int_0^{2\pi} \int_d^{d+h} \left| r^{\frac{1}{2}-|\gamma|} D^\gamma \mathbf{f}(\theta) \right|^2 r dr d\theta \\ &\leq \text{Max} [ |D^\gamma \mathbf{f}(\theta)|^2 ] \int_d^{d+h} r^{2-2|\gamma|} dr \\ &\leq \text{Max} [ |D^\gamma \mathbf{f}(\theta)|^2 ] d^{2-2|\gamma|} (d+h-d). \end{aligned} \tag{16}$$

Since  $d < 1$ ,

$$d^{2-2|\gamma|} h \leq d^{2-2(p+1)} h = d^{-2p} h \quad \text{for all } |\gamma| \leq p+1. \tag{17}$$

Using Eqs. (15)–(17) we get,

$$\begin{aligned} \|\mathbf{u}\|_{H^{p+1}(\Omega_e^*)}^2 &\leq \sum_{0 \leq |\gamma| \leq p+1} \text{Max} [ |D^\gamma \mathbf{f}(\theta)|^2 ] d^{2-2|\gamma|} h \\ &\leq \sum_{0 \leq |\gamma| \leq p+1} \text{Max} [ |D^\gamma \mathbf{f}(\theta)|^2 ] d^{-2p} h = C_1 d^{-2p} h \end{aligned} \tag{18}$$

where

$$C_1 = \sum_{0 \leq |\gamma| \leq p+1} \text{Max} [ |D^\gamma \mathbf{f}(\theta)|^2 ].$$

Therefore,

$$\|\mathbf{u}\|_{H^{p+1}(\Omega_e^*)}^2 \leq C_1 d^{-2p} h. \tag{19}$$

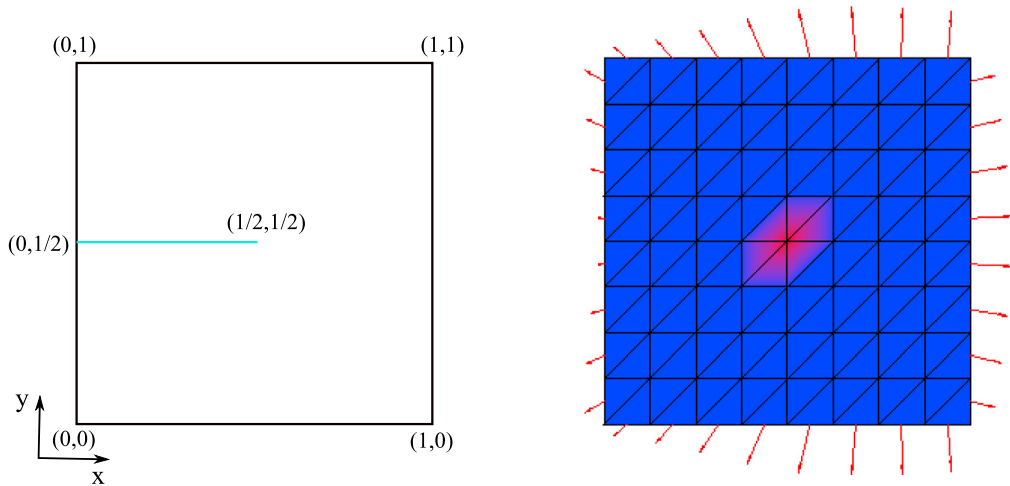


Fig. 6. Two-dimensional edge-cracked panel.

The convergence rate of the GFEM will be optimal if the right-hand-side of (19) is bounded by a constant, i.e.,

$$d^{-2p}h \leq C$$

$$Cd^{2p} \geq h.$$

Therefore, for optimal convergence rate, the size of the geometrical enrichment zone must satisfy

$$d \geq Ch^{\frac{1}{2p}}. \tag{20}$$

This estimate of the enrichment zone size is a function of the element size  $h$  and shape function polynomial order  $p$ . It shows that fine meshes require smaller enrichment zones for optimal convergence rate than coarse ones. In contrast, high-order shape functions require larger enrichment zones for optimal convergence than in the linear case. This is confirmed by the numerical experiments presented in Section 5. The estimate shows that the minimum size of the enrichment zone is not fixed and it decreases with mesh refinement. Therefore, if a fixed geometrical enrichment is adopted, which is the case found in the literature [24,23], an optimal convergence rate will be achieved with mesh refinement regardless of the value of the constant  $C$  in (20). This is also confirmed by the numerical experiments presented in Section 5. The element size required to achieve optimal convergence, however, may not be practical if  $d$  is small.

It is noted that estimate (20) holds in the case of linear elastic fracture mechanics problems with stress-free crack surfaces. Derivations for other types of boundary conditions on crack faces would follow the same steps. While the derivation was performed in a 2-D setting, the estimate is also applicable to *three-dimensional* problems *away from the boundary of the domain* since the strength of the singularity along a 3-D crack front is the same as in 2-D. Similar estimates can be derived for other classes of problems exhibiting singularities or strongly localized but finite gradients if their asymptotic solutions are known.

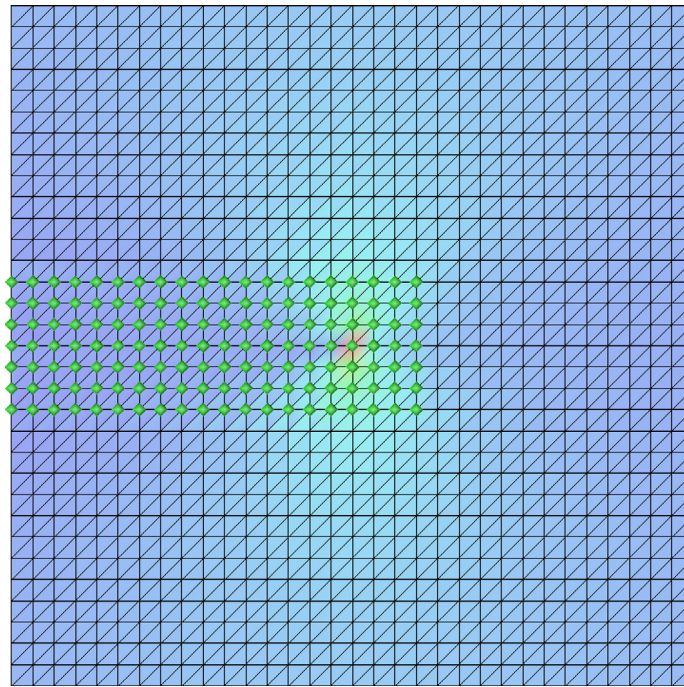
### 5. Numerical studies and discussion

Fig. 6 illustrates the 2-D linear elastic fracture mechanics problem used in the verification of estimate (20). It is an edge-cracked panel with the geometric dimensions shown in the figure and subjected to Neumann boundary conditions in the form of tractions  $\bar{\mathbf{t}}$ . Young's Modulus is taken equal to unity and a Poisson's ratio of 0.30 is adopted. Plane strain conditions are assumed to hold.

The traction vector  $\bar{\mathbf{t}}$  is computed from the first term of the Mode I expansion of the elasticity solution in the neighborhood of a crack:

$$\mathbf{u}_I(r, \theta) = \sqrt{r} \left\{ \begin{array}{l} \left( \kappa - \frac{1}{2} \right) \cos \frac{\theta}{2} - \frac{1}{2} \cos \frac{3\theta}{2} \\ \left( \kappa + \frac{1}{2} \right) \sin \frac{\theta}{2} - \frac{1}{2} \sin \frac{3\theta}{2} \end{array} \right\} \tag{21}$$

where  $r$  and  $\theta$  are polar coordinates at the crack tip,  $-\pi \leq \theta \leq \pi$ ,  $\kappa$  is a material constant  $(3 - 4\nu)$ , and  $\nu$  is the Poisson's ratio. Since (21) satisfies the equilibrium equations (1) and boundary conditions (2), it is the exact solution of the problem. This so-called *manufactured solution* is used to evaluate the convergence rate of the GFEM in the energy norm (4).



**Fig. 7.** Mesh corresponding to a  $32 \times 32$  rectangular grid. Diamond-shaped glyphs represent nodes enriched with singular functions in an enrichment zone of size  $d = 1/8$ .

The manufactured solution  $\mathbf{u}$ , given in (21) belongs to the Hilbert space of order  $k = 3/2$ . Therefore, the convergence rate in the energy norm of the FEM on a sequence of uniform meshes is equal to  $1/2$ , according to (9). This is also the case for the GFEM if topological enrichment is adopted or if only polynomial functions are used for the basis of the local spaces  $\chi_\alpha$ ,  $\alpha \in I_h^e$ . Our goal is to achieve optimal convergence rate given by the polynomial order  $p$  of the shape functions. This can be accomplished using geometrical enrichment, as discussed in previous sections. Linear and quadratic GFEM shape functions defined on uniform meshes as described below are adopted. In the first case, the polynomial GFEM shape functions are just the finite element partition of unity functions  $N_\alpha$ ,  $\alpha \in I_h$ . Quadratic GFEM shape functions are defined as [6,15],

$$N_\alpha \times \left\{ \frac{(x - x_\alpha)}{h_\alpha}, \frac{(y - y_\alpha)}{h_\alpha} \right\} \quad (22)$$

where  $h_\alpha$  is a scaling factor given by the diameter of the largest element sharing node  $\mathbf{x}_\alpha = (x_\alpha, y_\alpha)$ . These shape functions, together with the partition of unity, span quadratic polynomials over a finite element [15]. In addition to these polynomials, singular enrichments are adopted near the crack line as described below. They are used with both linear and quadratic GFEM shape functions.

Four finite element meshes are used in the convergence studies:  $64 \times 64$ ,  $128 \times 128$ ,  $256 \times 256$ , and  $512 \times 512$  grid of elements. The meshes are created by first generating a uniform mesh of quadrilateral elements and then dividing each element into two triangular elements. One of the meshes, corresponding to a  $32 \times 32$  grid of elements is shown in Fig. 7. The meshes in this study are selected such that the crack lies along the boundary of elements and the crack tip is at a node. This is done to facilitate the use of a special integration scheme for the singular GFEM shape functions. The integration rules proposed in [33] are adopted. It is to be noted, however, that the conclusions drawn from this study about the enrichment zone size are not affected by the location of the crack surface with respect to the mesh.

In the computations, singular enrichment functions defined from the Cartesian components of vector-valued function (21) and the first term of the Mode II expansion of the elasticity solution in the neighborhood of a crack

$$\mathbf{u}_{II}(r, \theta) = \sqrt{r} \begin{Bmatrix} \left( \kappa + \frac{3}{2} \right) \sin \frac{\theta}{2} + \frac{1}{2} \sin \frac{3\theta}{2} \\ \left( \kappa - \frac{3}{2} \right) \cos \frac{\theta}{2} + \frac{1}{2} \cos \frac{3\theta}{2} \end{Bmatrix}, \quad (23)$$

are used in the singular enrichment zone defined below. It is noted that enrichment functions given by (21) are sufficient for this problem since it is the exact solution. However, our implementation requires the use of both (21) and (23) as enrichment functions. The singularity at the crack tip and the discontinuity of the elasticity solution across the crack line



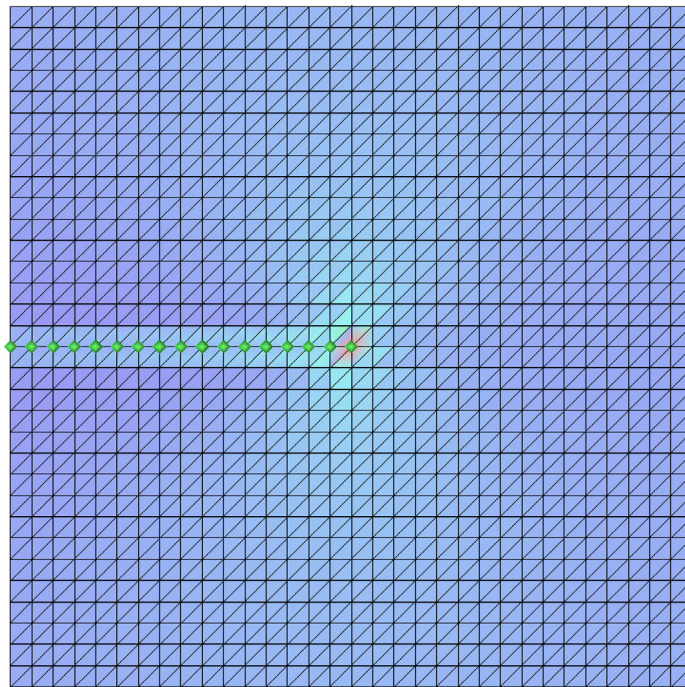


**Fig. 9.** Mesh corresponding to a  $32 \times 32$  rectangular grid illustrating topological enrichment scheme. Diamond-shaped glyphs represent nodes enriched with singular functions.

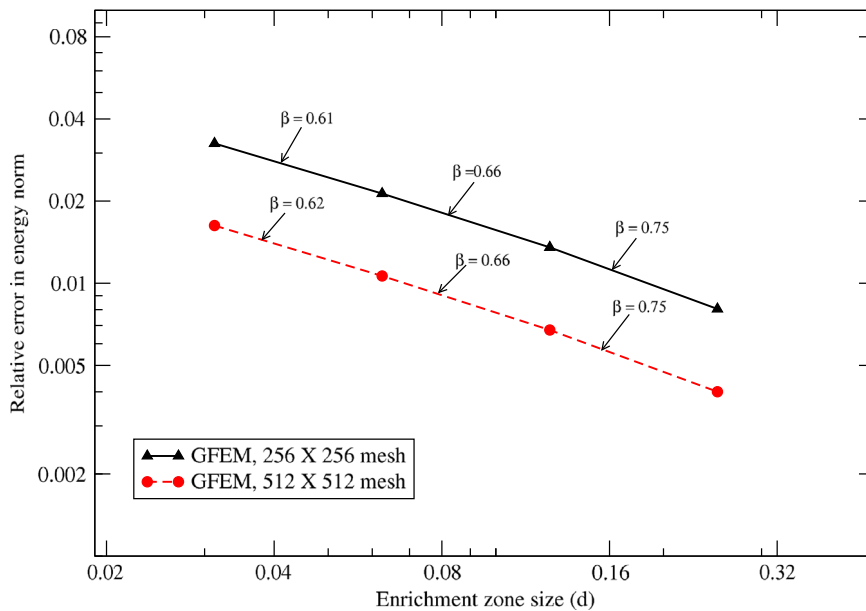


**Fig. 10.** Variation of error with the enrichment zone size for two meshes. Parameter  $\beta$  denotes the rate of convergence.

Fig. 12 shows convergence plots for the case of quadratic GFEM shape functions defined in (22). Singular enrichments are used as in the linear case discussed above. It can be observed that none of the enrichment zone sizes leads to an optimal convergence rate. Similar suboptimal convergence behavior is reported in the literature [23]. Nevertheless, the convergence rate increases with mesh refinement and a constant enrichment zone size  $d$ , which is consistent with estimate (20). However, much finer meshes are required to attain the optimal convergence behavior in the case of a higher polynomial approximation order, as predicted by the estimate (20). It is noted that in a generic fracture mechanics problems, additional singular enrichments based on the second term of the asymptotic expansion of the elasticity solution must also be used in order to achieve optimal convergence rate in the case of quadratic GFEM approximations. The manufactured solution (21) is given

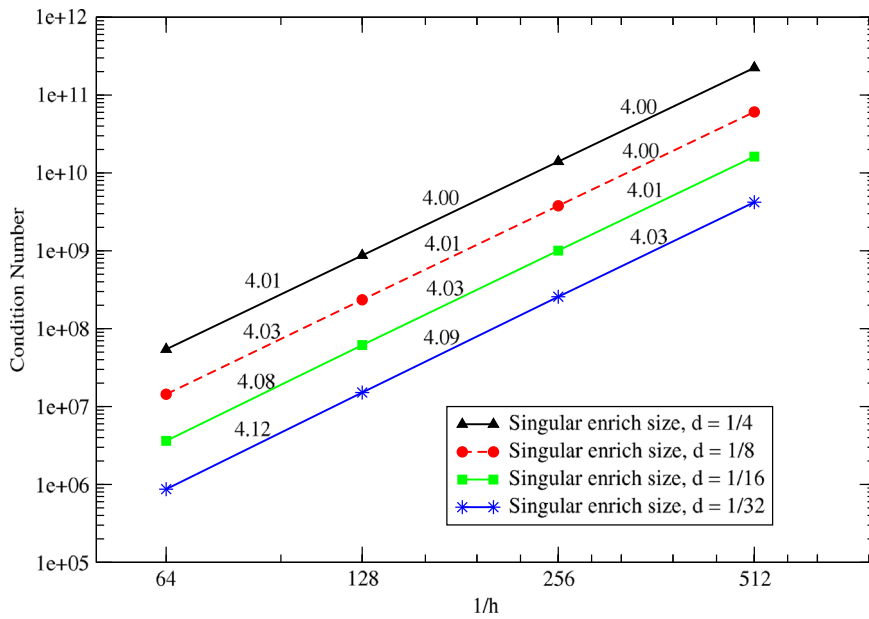


Fig. 11. Condition number of the stiffness matrix plotted against the inverse of element size for the case of linear approximation.

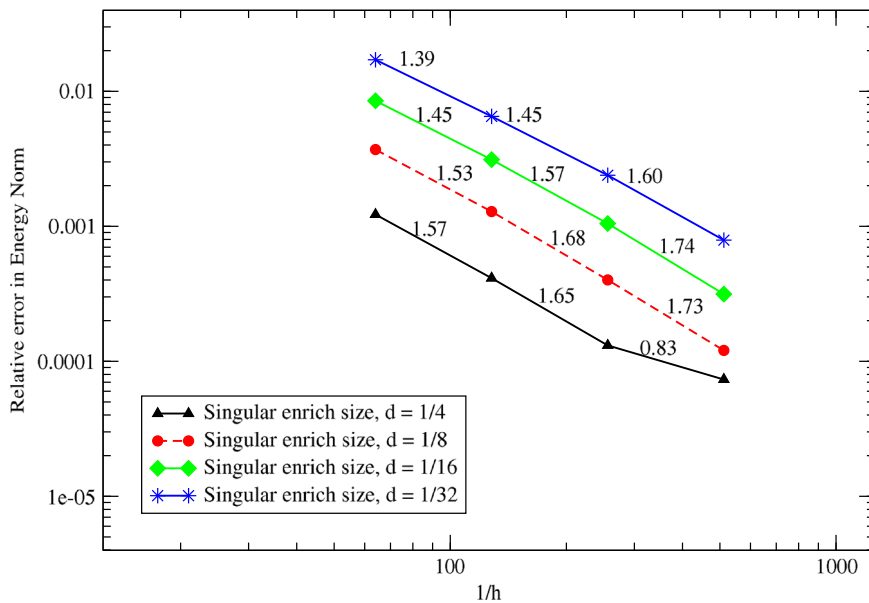


Fig. 12. Convergence plot for different enrichment zone sizes and quadratic GFEM shape functions.

by the first term of the asymptotic expansion and thus additional singular enrichments are not required to achieve optimal convergence even in the case of quadratic or higher-order GFEM approximations.

The last data point of the plot for  $d = 1/4$  shows a sudden reduction in the convergence rate. This point corresponds to the finest mesh and the largest enrichment size considered here and this anomalous behavior is likely caused by ill-conditioning of the stiffness matrix. The corresponding data point for the scaled condition number obtained with linear polynomial and singular GFEM shape functions is already available in Fig. 11. A detailed study focused on the numerical conditioning of GFEM approximations is provided in [28,35,36].

### 6. Concluding remarks

This study focuses on estimates for the size of enrichment zones that lead to optimal convergence rate of the GFEM on uniform meshes and elasticity problems with singularities. The results and conclusions drawn from this study can be summarized as follows:

- Geometrical enrichment zones are necessary to obtain optimal convergence rate in the GFEM/XFEM for fracture problems as demonstrated numerically in [24,23]. The topological enrichment strategy, which is broadly used in the literature and in particular when solving 3-D problems, leads to suboptimal convergence behavior.
- Large geometrical enrichment zones lead to a high number of degrees of freedom and ill-conditioned stiffness matrices. This provided the motivation for deriving an estimate of the minimum size of the enrichment zone able to deliver optimal convergence rate. To the authors' knowledge, this type of estimate has not been reported in the literature.
- The *a priori* estimate for the optimal size of the enrichment zone given by Eq. (20) can be used to guide the selection of the enrichment zones in the GFEM for 2- and 3-D fracture mechanics problems. Estimates for other classes of problems can also be derived, provided the asymptotic behavior of the solution near singularities is known.
- The proposed estimate shows that the size of the enrichment zone required for optimal convergence decreases with mesh refinement and increases with the polynomial order of the approximation. The results presented in Section 5 provide numerical evidence for such behavior.
- The estimate also provides a possible explanation for the observed suboptimal convergence rate in the case of high polynomial order GFEM/XFEMs reported in the literature [23] and also shown in Section 5.

## Acknowledgments

We thank Professor Hae-Soo Oh of the Department of Mathematics and Statistics, University of North Carolina at Charlotte, for fruitful discussions on certain aspects of this paper. The support from the US Air Force Office of Scientific Research under contract number FA9550-12-1-0379 is also gratefully acknowledged.

## References

- [1] I. Babuška, J.M. Melenk, The partition of unity method, *Internat. J. Numer. Methods Engrg.* 40 (1997) 727–758.
- [2] C.A.M. Duarte, J.T. Oden, An hp adaptive method using clouds, *Comput. Methods Appl. Mech. Engrg.* 139 (1996) 237–262. [http://dx.doi.org/10.1016/S0045-7825\(96\)01085-7](http://dx.doi.org/10.1016/S0045-7825(96)01085-7).
- [3] C.A.M. Duarte, J.T. Oden, Hp clouds—A meshless method to solve boundary-value problems. Technical Report 95-05, TICAM, The University of Texas at Austin, 1995.
- [4] C.A.M. Duarte, J.T. Oden, Hp clouds—An hp meshless method, *Numer. Methods Partial Differential Equations* 12 (1996) 673–705. [http://dx.doi.org/10.1002/\(SICI\)1098-2426\(199611\)12:6<protect>\relax\(\\$673::AID-NUM3<protect>\relax\)\\$3.0.CO2-P](http://dx.doi.org/10.1002/(SICI)1098-2426(199611)12:6<protect>\relax($673::AID-NUM3<protect>\relax)$3.0.CO2-P).
- [5] I. Babuška, G. Caloz, J.E. Osborn, Special finite element methods for a class of second order elliptic problems with rough coefficients, *SIAM J. Numer. Anal.* 31 (4) (1994) 945–981.
- [6] J.T. Oden, C.A. Duarte, O.C. Zienkiewicz, A new cloud-based hp finite element method, *Comput. Methods Appl. Mech. Engrg.* 153 (1998) 117–126. [http://dx.doi.org/10.1016/S0045-7825\(97\)00039-X](http://dx.doi.org/10.1016/S0045-7825(97)00039-X).
- [7] J.M. Melenk, I. Babuška, The partition of unity finite element method: Basic theory and applications, *Comput. Methods Appl. Mech. Engrg.* 139 (1996) 289–314.
- [8] N. Moës, J. Dolbow, T. Belytschko, A finite element method for crack growth without remeshing, *Internat. J. Numer. Methods Engrg.* 46 (1999) 131–150.
- [9] T. Belytschko, T. Black, Elastic crack growth in finite elements with minimal remeshing, *Internat. J. Numer. Methods Engrg.* 45 (1999) 601–620.
- [10] M. Griebel, M.A. Schweitzer, A particle-partition of unity method for the solution of elliptic, parabolic and hyperbolic PDEs, *SIAM J. Sci. Comput.* 22 (3) (2000) 853–890.
- [11] M.A. Schweitzer, Stable enrichment and local preconditioning in the particle-partition of unity method, *Numer. Math.* 118 (1) (2011) 137–170. <http://dx.doi.org/10.1007/s00211-010-0323-6>.
- [12] Abaqus, Version 6.11 Documentation. Dassault Systemes Simulia Corporation, Providence, RI, USA, 2011.
- [13] LS-DYNA, LS-DYNA user's manual. Livermore Software Technology Corporation, Livermore, CA, USA, 2013.
- [14] T. Belytschko, R. Gracie, G. Ventura, A review of extended/generalized finite element methods for material modeling, *Modelling Simul. Mater. Sci. Eng.* 17 (2009) 043001. <http://dx.doi.org/10.1088/0965-0393/17/4/043001>.
- [15] C.A. Duarte, I. Babuška, J.T. Oden, Generalized finite element methods for three dimensional structural mechanics problems, *Comput. Struct.* 77 (2000) 215–232. [http://dx.doi.org/10.1016/S0045-7949\(99\)00211-4](http://dx.doi.org/10.1016/S0045-7949(99)00211-4).
- [16] J.P. Pereira, C.A. Duarte, Extraction of stress intensity factors from generalized finite element solutions, *Eng. Anal. Bound. Elem.* 29 (2005) 397–413. <http://dx.doi.org/10.1016/j.enganabound.2004.09.007>.
- [17] R. Huang, N. Sukumar, J.H. Prevost, Modeling quasi-static crack growth with the extended finite element method Part II: Numerical applications, *Int. J. Solids Struct.* 40 (2003) 7539–7552.
- [18] S.E. Mousavi, E. Grinspun, N. Sukumar, Harmonic enrichment functions: A unified treatment of multiple, intersecting and branched cracks in the extended finite element method, *Internat. J. Numer. Methods Engrg.* 85 (10) (2011) 1306–1322. <http://dx.doi.org/10.1002/nme.3020>.
- [19] N. Sukumar, N. Moës, B. Moran, T. Belytschko, Extended finite element method for three-dimensional crack modelling, *Internat. J. Numer. Methods Engrg.* 48 (11) (2000) 1549–1570.
- [20] P.M.A. Areias, T. Belytschko, Analysis of three-dimensional crack initiation and propagation using the extended finite element method, *Internat. J. Numer. Methods Engrg.* 63 (2005) 760–788.
- [21] C.A. Duarte, O.N. Hamzeh, T.J. Liszka, W.W. Tworzydło, A generalized finite element method for the simulation of three-dimensional dynamic crack propagation, *Comput. Methods Appl. Mech. Engrg.* 190 (15–17) (2001) 2227–2262. [http://dx.doi.org/10.1016/S0045-7825\(00\)00233-4](http://dx.doi.org/10.1016/S0045-7825(00)00233-4).
- [22] J.P. Pereira, C.A. Duarte, D. Guoy, X. Jiao, Hp-Generalized FEM and crack surface representation for non-planar 3-D cracks, *Internat. J. Numer. Methods Engrg.* 77 (5) (2009) 601–633. <http://dx.doi.org/10.1002/nme.2419>.
- [23] P. Laborde, J. Pommier, Y. Renard, M. Salaün, High-order extended finite element method for cracked domains, *Internat. J. Numer. Methods Engrg.* 64 (2005) 354–381.
- [24] E. Béchet, H. Minnebo, N. Moës, B. Burgardt, Improved implementation and robustness study of the x-fem for stress analysis around cracks, *Internat. J. Numer. Methods Engrg.* 64 (2005) 1033–1056.
- [25] S. Nicaise, Y. Renard, E. Chahine, Optimal convergence analysis for the extended finite element method, *Internat. J. Numer. Methods Engrg.* 86 (2011) 528–548. <http://dx.doi.org/10.1002/nme.3092>.
- [26] J.E. Tarancón, A. Vercher, E. Giner, F.J. Fuenmayor, Enhanced blending elements for XFEM applied to linear elastic fracture mechanics, *Internat. J. Numer. Methods Engrg.* 77 (1) (2009) 126–148. <http://dx.doi.org/10.1002/nme.2402>.
- [27] T.P. Fries, A corrected XFEM approximation without problems in blending elements, *Internat. J. Numer. Methods Engrg.* 75 (5) (2008) 503–532. <http://dx.doi.org/10.1002/nme>.

- [28] V. Gupta, C.A. Duarte, I. Babuška, U. Banerjee, A stable and optimally convergent generalized FEM (SGFEM) for linear elastic fracture mechanics, *Comput. Methods Appl. Mech. Engrg.* 266 (2013) 23–39. <http://dx.doi.org/10.1016/j.cma.2013.07.010>.
- [29] V. Gupta, C.A. Duarte, I. Babuška, U. Banerjee, Stable GFEM (SGFEM): Improved conditioning and accuracy of GFEM/XFEM for three-dimensional fracture mechanics, *Comput. Methods Appl. Mech. Engrg.* 289 (2015) 355–386. <http://dx.doi.org/10.1016/j.cma.2015.01.014>.
- [30] B. Szabo, I. Babuška, *Finite Element Analysis*, John Wiley and Sons, New York, 1991.
- [31] J.T. Oden, J.N. Reddy, *An Introduction to the Mathematical Theory of Finite Elements*, John Wiley and Sons, New York, 1976.
- [32] C.A. Duarte, *The hp cloud method (Ph.D. dissertation)*, The University of Texas at Austin, Austin, TX, USA, 1996.
- [33] K. Park, J.P. Pereira, C.A. Duarte, G.H. Paulino, Integration of singular enrichment functions in the generalized/extended finite element method for three-dimensional problems, *Internat. J. Numer. Methods Engrg.* 78 (10) (2009) 1220–1257. <http://dx.doi.org/10.1002/nme.2530>.
- [34] MATLAB, version 8.3.0.532 (R2014a). The MathWorks Inc., Natick, MA, 2014.
- [35] I. Babuška, U. Banerjee, *Stable generalized finite element method (SGFEM)*, Technical Report ICES REPORT 11–07, The Institute for Computational Engineering and Sciences, The University of Texas at Austin, 2011.
- [36] I. Babuška, U. Banerjee, Stable generalized finite element method (SGFEM), *Comput. Methods Appl. Mech. Engrg.* 201–204 (2012) 91–111. <http://dx.doi.org/10.1016/j.cma.2011.09.012>.